Journal of Medicinal Chemistry

Article

Parallel Solution-Phase and Microwave-Assisted Synthesis of New *S*-DABO Derivatives Endowed with Subnanomolar Anti-HIV-1 Activity

Fabrizio Manetti, Jos A. Est, Imma Clotet-Codina, Mercedes Armand-Ugn, Giovanni Maga, Emmanuele Crespan, Reynel Cancio, Claudia Mugnaini, Cesare Bernardini, Andrea Togninelli, Caterina Carmi, Maddalena Alongi, Elena Petricci, Silvio Massa, Federico Corelli, and Maurizio Botta

J. Med. Chem., **2005**, 48 (25), 8000-8008• DOI: 10.1021/jm050744t • Publication Date (Web): 11 November 2005

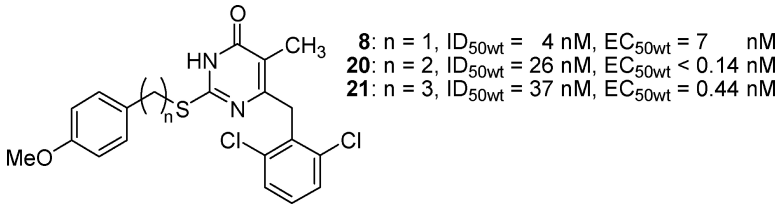

8: n = 1, ID_{50wt} = 4 nM, EC_{50wt} = 7 nM
20: n = 2, ID_{50wt} = 26 nM, EC_{50wt} < 0.14 nM
21: n = 3, ID_{50wt} = 37 nM, EC_{50wt} = 0.44 nM

More About This Article

Additional resources and features associated with this article are available within the HTML version:

- Supporting Information
- Links to the 6 articles that cite this article, as of the time of this article download
- Access to high resolution figures
- Links to articles and content related to this article
- Copyright permission to reproduce figures and/or text from this article

View the Full Text HTML

Journal of Medicinal Chemistry is published by the American Chemical Society. 1155 Sixteenth Street N.W., Washington, DC 20036

Parallel Solution-Phase and Microwave-Assisted Synthesis of New *S*-DABO Derivatives Endowed with Subnanomolar Anti-HIV-1 Activity

Fabrizio Manetti,[†] José A. Esté,[‡] Imma Clotet-Codina,[‡] Mercedes Armand-Ugón,[‡] Giovanni Maga,[§] Emmanuele Crespan,[§] Reynel Cancio,[§] Claudia Mugnaini,[†] Cesare Bernardini,[†] Andrea Togninelli,[†] Caterina Carmi,[||] Maddalena Alongi,[†] Elena Petricci,[†] Silvio Massa,[†] Federico Corelli,[†] and Maurizio Botta*[,†]

Dipartimento Farmaco Chimico Tecnologico, Università degli Studi di Siena, Via Alcide de Gasperi 2, I-53100 Siena, Italy, Retrovirology Laboratory irsiCaixa, Hospital Universitari Germans Trias i Pujol, Universitat Autónoma de Barcelona, E-08916 Badalona, Spain, Istituto di Genetica Molecolare, IGM-CNR, Via Abbiategrasso 207, I-27100 Pavia, Italy, and Dipartimento Farmaceutico, Università degli Studi di Parma, Parco Area delle Scienze 27/A, I-43100 Parma, Italy

Received July 29, 2005

A simple and efficient methodology for the parallel solution-phase synthesis has been set up to obtain a series of thiouracils, in turn selectively *S*-benzylated under microwave irradiation to give new *S*-DABOs. Biological screening led to the identification of compounds with nanomolar activity toward both the highly purified recombinant human immunodeficiency virus type 1 (HIV-1) reverse transcriptase (RT) enzyme (wild-type and mutants) and wild-type (wt) and mutant HIV-1 strains. In particular, **20** was found to be the most potent *S*-DABO reported so far (ID_{50} = 26 nM toward the isolated wt enzyme) with subnanomolar activity toward both the wt and the pluriresistant virus (IRLL98) HIV-1 strain (EC_{50} < 0.14 nM and EC_{50} = 0.22 nM, respectively). Molecular modeling calculations were also performed to investigate the binding mode of such compounds onto the non-nucleoside reverse transcriptase inhibitor binding site and to rationalize the relationships between their chemical structure and activity values toward wt RT.

Introduction

The current therapy against the human immunodeficiency virus type 1 (HIV-1), the causative agent of acquired immunodeficiency sindrome (AIDS), is based on four classes of drugs: nucleoside reverse transcriptase inhibitors (NRTIs), non-nucleoside reverse transcriptase inhibitors (NNRTIs), protease inhibitors (PIs), and fusion inhibitor enfuvirtide. Although NRTIs are equally active against HIV-1 and HIV-2 reverse transcriptase (RT), acting at the catalytic site as DNA chain terminators,[1] NNRTIs are highly specific for HIV-1 and include more than 30 structurally different classes of molecules, such as nevirapine,[2] TIBO,[3] BHAP,[4] α-APA,[5] PETT,[6] HEPT,[7] TNK-651,[8] ITU,[9] DATA,[10] and DAPY[11−13] (Chart 1).

The HIV-1 RT is a multifunctional enzyme, consisting of subunits p66 and p51, responsible for the conversion of the single-stranded RNA viral genome into double-stranded DNA. Lacking a biological counterpart in the eukaryotic systems, RT is an attractive target for the development of selective inhibitors.

Studies carried out on crystal structures of different RT/NNRTI complexes suggest that NNRTIs share a common mode of action, binding the RT enzyme at an allosteric site corresponding to a hydrophobic pocket in p66, called the non-nucleoside inhibitor binding pocket (NNIBP). The NNIBP is located about 10 Å from the catalytic site in the p66 subunit, and only a small portion of it is formed by amino acid residues belonging to the p51 subunit.[8,14−21] During the process of inhibitor binding, significant conformational changes occur in the orientation of the side chains of some residues (particularly Tyr181 and Tyr188), leading to the formation of the NNIBP accommodating the inhibitors. It is evident from a comparison of the various RT structures that the NNIBP has a very flexible structure and this characteristic allows the enzyme to accommodate structurally diverse inhibitors that have different shapes and sizes.[22] Although NNRTIs generally exhibit low toxicity and favorable pharmacokinetic properties, the rapid replication of HIV and its inherent variability often lead to the generation of drug-resistant variants responsible for the clinical NNRTI treatment failure.[23−24]

Among NNRTIs, dihydro-alkoxy-benzyl-oxopyrimidines (DABOs) are an interesting class of compounds active at nanomolar concentration; they were first disclosed in 1992[25] and further developed during the following years into *S*-DABOs (Chart 1) and related analogues. Recently, we identified compounds **1** and **2** as byproducts of cleavage of thiopyrimidinones from Wang resin (Chart 1).[26] Considering their structural similarity to known *S*-DABOs, we tested these compounds as possible NNRTIs, and despite their moderate activity (IC_{50} = 400 μM), we became interested in investigating the influence of the arylalkyl moiety on anti-HIV activity because only scattered examples of *S*-DABOs having this kind of substitution at position 2 had been reported in the literature. Herein, we describe the microwave-assisted synthesis of new *S*-DABO derivatives **3**−**30**, endowed with anti-HIV activity at nanomolar or picomolar concentrations on cell lines infected with either wild-type or mutated HIV-1.

* Author to whom correspondence should be addressed. Phone: +39 0577 234306. Fax: +39 0577 2343330. E-mail: botta@unisi.it.
[†] Università degli Studi di Siena.
[‡] Universitat Autónoma de Barcelona.
[§] Istituto di Genetica Molecolare.
[||] On leave from the Università degli Studi di Parma.

10.1021/jm050744t CCC: $30.25
Published on Web 11/11/2005

Chart 1. Structure of Known NNRTIs

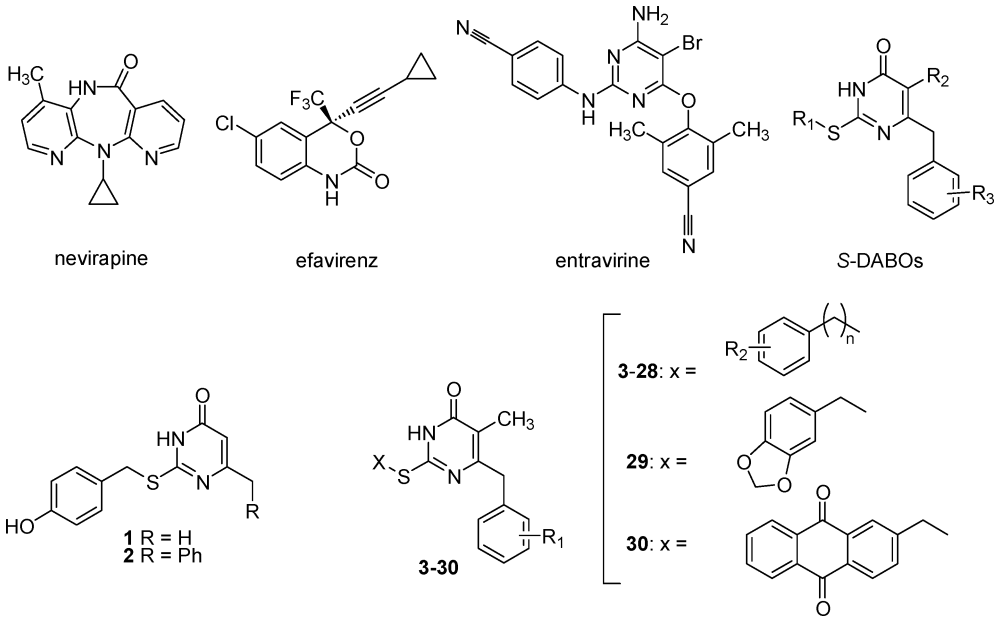

Scheme 1[a]

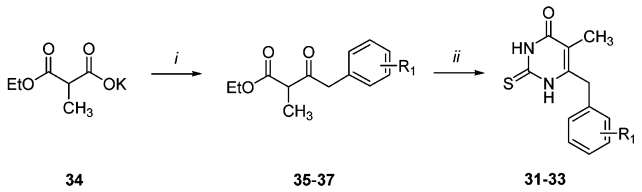

[a] Reagents and conditions: (i) a. $MgCl_2$, Et_3 N, CH_3CN, rt, 360 rpm, 2 h; b. substituted phenylacetic acid, *N*,*N*′-carbonyldiimidazole, rt, 360 rpm, overnight then reflux, 360 rpm, 2 h; c. 13% HCl, rt, 360 rpm, 10 min; (ii) thiourea, EtONa, reflux, 360 rpm, overnight.

Scheme 2[a]

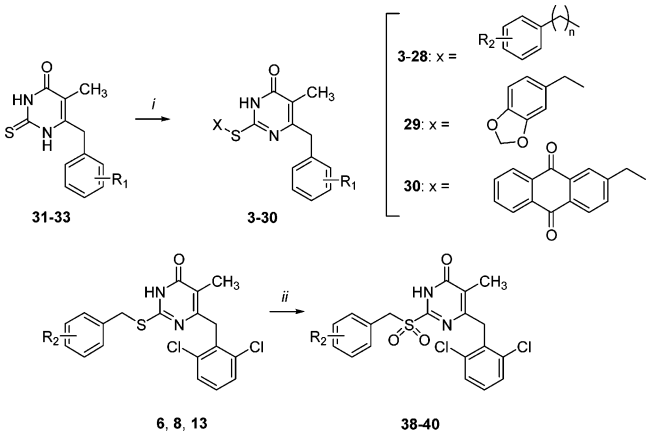

[a] Reagents and conditions: (i) substituted benzyl halide, DMF, MW, 130 °C, 5 min (method A) or substituted benzyl alcohol, trimethylphosphine, DIAD, DMF, MW, 40 °C, 10 min (method B); (ii) MCPBA, CH_2Cl_2, rt, 360 rpm, overnight.

In particular, starting from our lead compounds **1** and **2**, we planned to design a number of *S*-DABO derivatives characterized by the presence of (i) an arylalkylthio substituent at position 2 that represents the focus of our investigations. To expand the structure−activity relationships (SARs) of *S*-DABOs, the substitution pattern on the phenyl ring was broadly varied, as well as the length of the alkyl spacer, which was increased from one to three carbon atoms, (ii) a 5-methyl group, which was kept fixed in all the molecules, as a conformational constraint with the aim of enhancing the affinity for the enzyme, (iii) a halogenated benzyl group at the 6 position, which was expected to improve a putative π-stacking interaction between the electron-deficient benzene ring of the ligand and the electron-rich benzene ring of Tyr188 located in the NNBP of the enzyme.[27]

Chemistry

As an extension of our ongoing efforts toward the development of new methodologies for the synthesis of pyrimidine and pyrimidinone derivatives[28] and in view of a more extensive functionalization of the positions 5 and 6 of the thiopyrimidinone scaffold, we have set up a simple and efficient methodology for the parallel solution-phase synthesis of thiouracils **31**−**33** using a Büchi Syncore synthesizer (Scheme 1). Potassium ethyl 2-methylmalonate (**34**) was partitioned into three reaction vessels and reacted with three substituted phenylacetyl imidazolides in the presence of a magnesium dichloride/triethylamine system in acetonitrile according to the Clay procedure[29] to give, after a simple liquid-phase extractive purification, the β-keto esters **35**−**37**. Subsequent condensation of **35**−**37** with thiourea in the presence of sodium ethoxide in refluxing ethanol afforded 6-benzyl-2,3-dihydro-5-methyl-2-thioxopyrimidin-4(1*H*)-ones (**31**−**33**).

Exploitation of this procedure might allow the rapid synthesis of a large number of *S*-DABO derivatives variously substituted at positions 2, 5, and 6 for further SAR studies in this class of compounds.

5,6-Disubstituted thiouracils **31**−**33** were selectively *S*-benzylated under microwave irradiation with the appropriate substituted benzyl halide in dry DMF in the presence or not of potassium carbonate (Method A) (Scheme 2).[30] Alternatively, **31**−**33** were *S*-benzylated using the appropriate benzyl alcohol via a microwave-assisted Mitsunobu reaction in the presence of trimethylphosphine and diisopropylazodicarboxylate (DIAD) in

Table 1. Chemical and Physical Data of Derivatives **3**−**30** and **38**−**40**

cmpd	R_1	R_2	*n*	mp (°C)	recryst solvent	yield (%)	method of synthesis
3	2,6-diCl	H	1	236−237	CH_3CN	50	A
4	2,6-diCl	4-F	1	205−206	CH_3CN	50	A
5	2,6-diCl	4-Cl	1	214	CH_3CN	65	A
6	2,6-diCl	4-Br	1	219	CH_3CN	67	A
7	2,6-diCl	4-OH	1	204−206	CH_3CN	64	B
8	2,6-diCl	4-OCH_3	1	197−199	CH_3CN	72	A
9	2,6-diCl	4-OCH_2CH_3	1	218−221	CH_3CN	73	B
10	2,6-diCl	4-OBu	1	201−205	CH_3CN	79	B
11	2,6-diCl	4-*i*Pr	1	221−223	CH_3CN	60	A
12	2,6-diCl	4-CN	1	232−235	CH_3CN	78	A
13	2,6-diCl	4-NO_2	1	231−232	CH_3CN	55	A
14	2,6-diCl	3-F	1	238−239	CH_3CN	50	A
15	2,6-diCl	3-Cl	1	232	CH_3CN	51	A
16	2,6-diCl	3-CN	1	203	CH_3CN	77	A
17	2,6-diCl	2,4-diOCH_3	1	217−219	$CH_3OH/CHCl_3$	72	B
18	2,6-diCl	3,4-diOCH_3	1	195−196	$CH_3OH/CHCl_3$	65	B
19	2,6-diCl	3,5-diOCH_3	1	246−247	CH_2Cl_2	50	A
20	2,6-diCl	4-OCH_3	2	182−183	CH_3CN	53	B
21	2,6-diCl	4-OCH_3	3	180−182	CH_3CN	67	B
22	2,6-diF	4-OCH_3	1	170−171	CH_3CN	52	A
23	2,6-diF	4-*i*Pr	1	179−181	CH_3OH/CH_3CN	49	A
24	2,6-diF	4-CN	1	247−248	CH_3CN	57	A
25	2,6-diF	4-NO_2	1	248−250	CH_3CN	40	A
26	2,6-diF	3,5-diOCH_3	1	228−230	CH_3CN	59	A
27	4-F	4-NO_2	1	246	CH_3CN	56	A
28	4-F	4-OCH_3	1	190	CH_3CN	63	A
29	2,6-diCl		1	192−194	CH_3CN/CH_2Cl_2	58	B
30	2,6-diCl		1	>250	$CH_3OH/CHCl_3$	69	B
38	2,6-diCl	4-OCH_3	1	171−174	CH_3CN	71	
39	2,6-diCl	4-NO_2	1	175−180	CH_3CN	55	
40	2,6-diCl	4-Br	1	241−244	CH_3CN	50	

dry DMF (Method B). In both cases, the use of microwaves allowed us to obtain, in a few minutes, the desired products in high yield and good purity.

Finally, sulfides **6**, **8**, and **13** were oxidized to sulfones **38**−**40** with *m*-chloroperbenzoic acid in dichloromethane at room temperature.[31]

All of the compounds were obtained in more than 95% purity, as shown by HPLC−MS analysis. Chemical and physical data of the new compounds are reported in Table 1.

Results and Discussion

Title compounds **3**−**30** and **38**−**40**, a new family of *S*-DABOs characterized by the presence of an arylalkylthio substitution at C-2, a methyl group at C-5, and a halogenated benzyl group at C-6 of the pyrimidinone nucleus, were prepared in a straightforward fashion by alkylation of three different 6-substituted 2-thiouracils (**31**−**33**) and subsequent oxidation of the sulfur atom (**38**−**40**).

The new compounds were evaluated in enzymatic tests for their ability to inhibit either wild-type (wt) or mutated RTs as well as on MT-4 cells for cytotoxicity and anti-HIV-activity, in comparison with nevirapine and efavirenz, used as reference drugs. In particular, the following mutants were used: K103N and Y181I for enzymatic tests, K103N, Y188L, and pluriresistant virus (IRLL98) (bearing the K101Q, Y181C, and G190A mutations conferring resistance to nevirapine, delavirdine, and efavirenz, respectively) for tests on cell lines. The results of these assays are reported in Table 2. Moreover, Table 3 reports fold-resistance values of selected compounds against a panel of mutant strains, in comparison to those of AZT, nevirapine, and efavirenz.

Although previous findings obtained with other *S*-DABO series highlighted the importance for optimal activity of a 2,6-difluorobenzyl substituent at position 6,[32] in our case this type of substitution proved to be less profitable with respect to the corresponding 2,6-dichlorobenzyl group. In fact, although compound **8** was highly active both in enzymatic and cell tests, showing appreciable activity also against IRLL98, compound **22** retained activity only against the wt RT. Moreover, a striking difference in activity can be observed between that of **13** (displaying a full-range activity at low concentrations so as to emerge as one of the most interesting compounds of the series) and that of **25**, whose activity was limited to wt virus and unrelated to RT inhibiting properties. In line with these observations, the presence of a 6-(4-fluorobenzyl) group led to the substantially inactive compounds **27** and **28**.

On the basis of these results, we kept the 6-(2,6-dichlorobenzyl) substituent fixed and systematically modified the C-2 position. The 4-hydroxybenzyl group, found in our lead compounds **1** and **2** and also present in compound **7**, did not positively contribute to the antiviral activity. Replacement of the OH group with H, F, Cl, Br, *i*Pr, and CN improved the general biological profile (compounds **3**−**6**, and **12**), with activity ranging from 0.39 to 103 μM in enzymatic tests, and from 0.11 to 0.83 μM on cells infected with wt virus. No interesting activity was observed on mutant strains, with the exception of **12**, which retained activity on clinically relevant mutants at a micromolar or submicromolar concentration. Moving the substituent (F, Cl, CN) from a para to a meta position on the aromatic ring did not modify the biological response to the molecules (**14**−**16**). On the other hand, replacement of the OH group with NO_2 led to the very interesting compound **13** (vide supra), whereas substitution of the OH group with alkoxy groups gave compounds **8**−**10**, whose activities were strongly dependent on the length of the alkyl

Table 2. Anti HIV-1 Activity and Cytotoxicity of Compounds **3**−**30** and **38**−**40**

	ID_{50} (μM)[a,b]			EC_{50} (μM)[a,c]				
cmpd	wt	K103N	Y181I	NL4−3 wt	IRLL98	K103N	Y188L	CC_{50}[f]
3	2.5	350	na[d]	0.83	>64	>64	>64	>64
4	16	na	na	0.11	2.7	27	>61	>61
5	20	na	na	0.47	2.1	>59	>59	>59
6	0.39	9	na	0.79	>53	>53	>53	13
7	na	na	na	>41	>41	>41	>41	41
8	0.004	102	150	0.007	0.047	4.7	>32	32
9	2	na	na	0.25	1.9	>58	>58	>58
10	2.8	na	na	>3.1	34% at 11[e]	>3.1	>3.1	3.1
11	na	na	na	35% at 2.3	>57	>58	>58	45% at 11
12	103	na	na	0.17	1.0	0.10	>60	>60
13	0.009	0.12	0.22	0.79	3.3	11	31%	>58
14	2.0	35	na	0.15	2.2	>61	>61	>61
15	2.3	400	400	0.31	4.8	>59	>59	>59
16	9.5	na	na	0.89	5.0	>60	>60	>60
17	25	na	na	1.33	>55	>55	>55	>55
18	1.2	na	na	0.20	0.93	10	>55	>55
19	256	na	na	33	>55	>55	>55	>55
20	0.026	3.2	1.5	<0.00014	0.00022	0.87	6.9	>57
21	0.037	0.5	0.3	0.00044	0.11	>1.0	>1.0	1.0
22	0.007	3.5	na	0.026	0.69	0.69	10	>64
23	3	na	na	0.58	16	33% at 62	>62	>62
24	0.76	na	na	0.052	>65	>65	>65	>65
25	na	na	na	0.074	>62	>62	>62	>62
26	na	na	na	18	>60	>60	>60	>60
27	na	na	na	>65	>65	>65	>65	>65
28	na	na	na	>8.9	>8.9	>8.9	>8.9	8.9
29	0.5	na	na	0.12	0.51	5.3	33	>57
30	3.5	na	na	13	>48	>48	>48	>48
38	0.006	10	27	>2.8	>2.8	>2.8	>2.8	2.8
39	na	na	na	>53	>53	>53	>53	>53
40	na	na	na	>50	>50	>50	>50	>50
nevirapine	0.4	8	20	0.052	>7.5	3.9	>7.5	>7.5
efavirenz	0.04	0.4	0.1	0.001	0.2	0.057	0.3	>0.32
AZT				0.003	0.008	0.003	0.003	3.7

[a] Data represent mean values of at least two experiments. [b] ID_{50}: Inhibiting dose 50 or needed dose to inhibit 50% of enzyme. [c] EC_{50}: Effective concentration 50 or needed concentration to inhibit 50% HIV-induced cell death, evaluated with MTT method in MT-4 cells. [d] na: Not active at 400 μM (the highest concentration tested). [e] Percent inhibition of HIV-induced cell death at the reported micromolar concentration. [f] CC_{50}: Cytotoxic concentration 50 or needed concentration to induce 50% death of noninfected cells evaluated with the MTT method in MT-4 cells.

Table 3. Fold Resistance Values of Selected Compounds Against a Panel of Mutant Strains, in Comparison to Those of AZT, Nevirapine, and Efavirenz

	EC_{50} (μM)	fold resistance		
cmpd	toward NL4-3 wt	IRLL98	K103N	Y188L
8	0.007	7	670	3000
12	0.17	6	0.5	>60.1
13	0.79	3.31	10.64	31%
16	0.89	5	>67.5	>67.5
18	0.20	4.6	51.2	>276
22	0.026	20.08	20.63	302.71
29	0.12	4.4	45.5	283.5
AZT	0.003	3	1	1
NVP	0.052	144	70	144
EVZ	0.001	300	80	400

moiety. Thus, whereas **9** and **10** (*p*-ethoxy and *p*-butoxy groups, respectively) were only moderately active on the wt, compound **8** (*p*-methoxy) was endowed with very significant activity in the nanomolar range toward both wt and IRLL98 strains, as well as with low toxicity (SI > 4600). The contemporary presence on the aromatic ring of more than one methoxy group negatively affected the biological activity. In particular, although a modest effect on wt RT can still be ascribed to compounds **17**, **18**, and **29** (having a substituent at the para position), no interesting activity was demonstrated by **19** and **26** (R = 3,5-dimethoxyphenyl). Even more detrimental to antiviral activity was the presence of a bulky group on the aryl moiety, as in compounds **11**, **23**, and **30**.

A very marked improvement of the biological profile was obtained by increasing the length of the linker connecting the aromatic ring to the sulfur atom. Compounds **20** and **21** (n = 2 and 3, respectively) proved to be the most interesting among the new derivatives. In particular, **20** exhibited anti-HIV activity on cells infected with either wild-type or pluriresistant virus (IRLL98) at subnanomolar concentration, together with low cytotoxicity (SI > 410 000). On the whole, this compound showed an anti-HIV profile superior to that of nevirapine and comparable to that of efavirenz, thus emerging as the most active *S*-DABO analogue reported so far. Further lengthening of the linker led to compound **21** that, though retaining very good anti-HIV activity, was endowed with higher cytotoxicity. Finally, basically inactive compounds (**38**−**40**) were obtained by oxidation of the sulfur atom.

Biological data showed some contradictions between ID_{50} and EC_{50} values for several compounds, probably due to the fact that cellular tests reflect the interference of a compound in viral steps not shown in the pure RT enzymatic tests (i.e., enzymatic tests account only for the DNA−RNA-dependent synthesis inhibition, whereas cellular test results represent the inhibition of all viral replication phases). Moreover, we cannot exclude the possibility that the low cellular activity or the inactivity

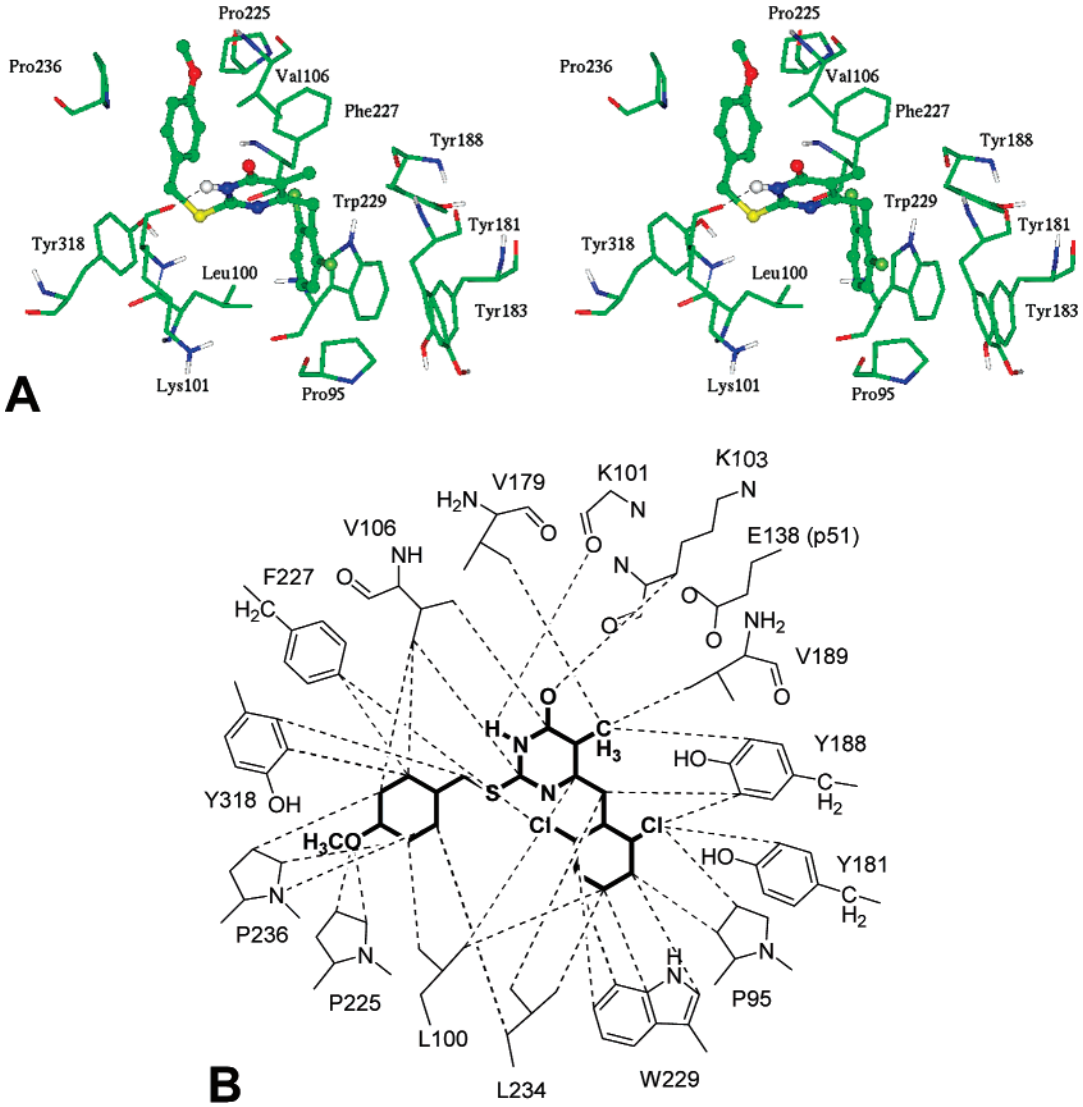

Figure 1. Stereographic (A, the inhibitor shown in ball-and-stick notation) and schematic (B, the inhibitor drawn with thick lines) representations of the orientation mode of compound **8** into the NNIBD. The terminal methyl group of the side chain at position 2 contacts both Pro225 and Pro236 at the surface of RT. Moreover, the 3-NH group of the pyrimidinone ring is involved in a hydrogen-bond interaction with the carbonyl oxygen of Lys101. Finally, the benzyl chain at position 6 is accommodated within a large pocket mainly defined by the hydrophobic side chains of Leu100, Trp229, Phe227, Tyr181, Tyr183, and Tyr188. For sake of clarity, only representative amino acids are shown.

of some of our compounds could be the consequence of poor adsorption through the T-cell membrane, in addition to a poor affinity for the corresponding receptor counterpart.

Molecular Modeling Calculations

To investigate the binding mode of the new RT inhibitors, molecular-docking simulations were performed by means of the software Autodock. Results showed **8** assuming an orientation very similar to that of the cocrystallized inhibitor (MKC-442, emivirine). In particular, the pyrimidinone ring of **8** was superposable to that of MKC-442, allowing for a hydrogen-bond contact between its NH group at position 3 with the carbonyl moiety of Lys101 (1.9 Å), suggested to be a crucial interaction key for inhibitors belonging to the DABO and *S*-DABO classes of compounds.[32] Moreover, the side chains of both Lys103 and Val106 were also found at close contact with the pyrimidinone nucleus. The extended side chains at position 2 of both **8** and MKC-442 were lined up in a parallel way and pointed toward the solvent-accessible surface defined by Pro225 and Pro236. In further detail, although the sulfur atom of **8** was located at a distance of about 3.7 Å from the backbone-NH group of Lys101, the benzyl moiety was accommodated into a large pocket mainly defined by Val106, Pro225, Pro236, and Tyr318 (Figure 1). Good profitable hydrophobic interactions were found between the alkyl side chain of Val106 and the phenyl ring of the inhibitor as well as between the terminal methyl group with both Pro225 and Pro236. Finally, the benzyl substituent at position 6 of **8** was embedded into an extended hydrophobic region defined by the aromatic side chains of Tyr181, Tyr188, Phe227, and Trp229 as well as by Leu100 and Leu234. The major difference between the experimental and calculated complexes involved the interaction between the 6-benzyl side chain of the inhibitors and the side chain of Trp229. In fact, although a T-tilted interaction was shown in the complex with MKC-442, a $\pi-\pi$ interaction was found in the complex with **8**. This was mainly due to the fact that a

significant conformational rearrangement occurred within the aromatic cage accommodating the substituent at position 6. In fact, the aromatic side chains of Tyr183, Tyr188, and Trp229 approached the inhibitor, leading to a structural system where the indole nucleus was sandwiched between the 6-benzyl group of the inhibitor and the phenyl ring of Tyr183 (allowing $\pi-\pi$ interactions) and interacted with a T-tilted contact with the aromatic moiety of Tyr188. On the other hand, although Phe227 retained its original position, a rotation of the Tyr181 side chain occurred that pushed it about 1.8 Å away from the NNIBP.

Similar results were found for the nitro derivative **13**, with a major difference involving the benzylthio side chain that was located in a region of space comprised between the corresponding side chain of **8** and the N1 side chain of the crystallized inhibitor. In particular, due to a rotation of about 20° around the C2−S bond, the nitro group was inserted between Pro225 and the side chain of Phe227, and one of its electron-rich oxygen atoms was found at the proper distance (1.6 Å) to make a hydrogen-bond contact with the backbone-NH group of Phe227.

Lengthening the benzyl moiety of **8** to a phenylethyl (**20**) and phenylpropyl (**21**) chain led their *p*-methoxy group to go beyond the opening defined by Pro225 and Pro236 and, thus, to be exposed to the solvent. Moreover, such a shift of the phenyl ring caused the lack of its hydrophobic interactions with the side chain of Val106. The pyrimidinone nucleus of **21** maintained an orientation comparable to that of **8**, including the hydrogen-bond contact with Lys101 as well as the hydrophobic interactions with a part of the Val106 side chain. Similarly, no substantial difference was found for the location of the benzyl substituent at position 6, in comparison to that of **8** and the crystallized inhibitor. On the other hand, the 6-benzylpyrimidinone system of **20** underwent a significant conformational rearrangement, allowing for a hydrogen-bond contact involving the carbonyl oxygen and the backbone-NH group of Lys101, in addition to the hydrogen-bond contact between the 3-NH group of the inhibitor and the carbonyl of the same amino acid. Moreover, due to the fact that the benzyl group at the position 6 was characterized by an alternative orientation into the hydrophobic cage previously described, the profitable aromatic−aromatic interaction involving the side chain of Trp229 was lost.

In summary, docking calculations suggested that the *p*-methoxybenzylthio group at position 2 of **8** seems to be characterized by the optimal length to fulfill the tunnel delimited, at the surface of the RT structure, by Pro225 and Pro236. Moreover, the lower activity of **20** and **21** toward the wt RT, with respect to that of their shorter analogue **8**, was in part due to reduced hydrophobic interactions mainly involving the benzyl substituents at position 2 as well as to unfavorable contacts between the terminal methyl substituent and the solvent. In a similar way, analogues of **8**, bearing at the para position of the 2-benzyl substituent a hydrophobic group larger than a methoxy moiety (exceeding the surface of the RT and contacting the solvent), showed lower activity than **8**. In fact, the ethoxy, butoxy, and isopropyl derivatives (**9**, **10**, and **11**) showed activity in the micromolar range or lower.

Conclusions

Parallel solution-phase and microwave-assisted synthesis was applied to the synthesis of new *S*-DABO derivatives having a 2-phenylalkylthio side chain of variable length, characterized by different substituents and substitution patterns on the phenyl ring. Results from anti-HIV reverse transcriptase assays and anti-HIV activity in lymphoid cells showed activity values in the nanomolar and subnanomolar range, respectively. Moreover, one of the new compounds (**20**) was characterized by an anti-HIV profile better than that of nevirapine and comparable to that of efavirenz, thus emerging as the most active *S*-DABO analogue reported so far.

Experimental Section

Chemistry. Reagents were obtained from commercial suppliers and used without further purifications. According to standard procedures, CH_2Cl_2 was dried over calcium hydride, MeOH and EtOH were dried over Mg/I_2 prior to use, and DMF was bought already anhydrous. Anhydrous reactions were run under a positive pressure of dry N_2 or argon. IR spectra were recorded on a Perkin-Elmer BX FT-IR system using $CHCl_3$ as the solvent. TLC was carried out using Merck TLC plates Kieselgel 60 F_{254}. Chromatographic purifications were performed on columns packed with Merck 60 silica gel, 23−400 mesh, for flash technique. Melting points were taken using a Gallenkamp melting point apparatus and are uncorrected. ^{1}H NMR spectra were recorded with a Bruker AC200F spectrometer at 200 MHz, and chemical shifts are reported in δ values, relative to TMS at δ 0.00 ppm. CD_3OD, DMSO-d_6, and CD_3Cl were used as solvents. Buchi Syncore polyvap was used for parallel synthesis, filtration, and evaporation.

HPLC and MS Analysis. The purity of the compounds was assessed by reversed-phase liquid chromatography and mass spectrometry (Agilent series 1100 LC/MSD) with a UV detector at $\lambda = 254$ nm and an electrospray ionization source (ESI). The LC elution method (using Hypersil ODS, 4.6 mm × 200 mm, 5 μm C18 column; Zorbax Eclipse XDB, 4.6 mm × 150 mm, 5 μm C8 column) was the following: 20 min method at 25 °C, mobile phase composed of different MeOH/H_2O or CH_3CN/H_2O mixtures at a flow rate of 1 mL/min (all solvents were HPLC grade, Fluka). Mass spectral (MS) data were obtained using an Agilent 1100 LC/MSD VL system (G1946C) with a 0.4 mL/min flow rate using a binary solvent system of 95:5 MeOH/water. UV detection was monitored at 254 nm. Mass spectra were acquired in positive mode scanning over the mass range of 50−1500. The following ion source parameters were used: drying gas flow, 9 mL/min; nebulizer pressure, 40 psig; drying gas temperature, 350 °C.

Microwave Irradiation Experiments. Microwave reactions were conducted using a CEM Discover Synthesis Unit (CEM Corp., Matthews, NC). The machine consists of a continuous focused microwave-power delivery system with operator-selectable power output from 0 to 300 W. The temperature of the contents of the vessel was monitored using a calibrated infrared temperature control mounted under the reaction vessel. All experiments were performed using a stirring option whereby the contents of the vessel are stirred by means of a rotating magnetic plate located below the floor of the microwave cavity and a Teflon-coated magnetic stir bar in the vessel.

Synthesis. Parallel Synthesis of Ethyl 2-Methyl-4-substituted Phenyl-3-oxobutanoates (35−37). General Procedure. Potassium ethyl 2-methylmalonate[33] (**34**) (0.929 g, 5.04 mmol), placed in three different vessels of the Buchi Syncore, was suspended in dry acetonitrile (6 mL). Triethylamine (1.07 mL, 7.67 mmol) and magnesium chloride (0.571 g, 6 mmol) were added to the stirred suspensions and the mixtures stirred (360 rpm) at room temperature for 2 h. Then were added the solutions of (substituted phenylacetyl)imida-

zolides in dry acetonitrile, prepared 15 min before by reaction between appropriate phenylacetic acid (2.4 mmol) and *N,N′*-carbonyldiimidazole (0.427 g, 2.67 mmol) in acetonitrile (3 mL). The reaction mixtures were stirred (360 rpm) overnight at room temperature and then refluxed for 2 h. Six milliliters of 13% HCl was added dropwise to the cooled mixtures, and the resulting clear mixtures were stirred (360 rpm) for an additional 10 min. Finally, the organic layers were separated in parallel with a specific filtration unit. The aqueous phases were extracted once with ethyl acetate (10 mL), and the organic phases were combined and then evaporated to dryness in parallel with the same apparatus to give **35**−**37** as colorless oils to be used in the next step without further purification. Spectroscopic and analytical data for compounds **35**−**37** are in agreement with those reported in the literature.[27]

Parallel Synthesis of Substituted 6-Benzyl-5-methyl-3,4-dihydro-2-thioxopyrimidin-4(3*H*)-ones (31−**33). General Procedure.** Sodium (0.105 g, 4.55 mmol) was placed in three different vessels of the Buchi Syncore and dissolved in 8 mL of anhydrous ethanol under a positive pressure of dry N_2. Thiourea (0.241 g, 3.178 mmol) and **35**−**37** (2.27 mmol) were added in different vessels, and the resulting mixtures were shaken overnight at reflux temperature at 360 rpm. Then, solvent was evaporated in parallel, and the residues were redissolved in the least amount of water (3 mL). After neutralization with 0.5 N acetic acid, the products were extracted in parallel with ethyl acetate (3 × 10 mL). The organic phases, separated with a specific filtration unit, were combined and evaporated to dryness with the same apparatus. Finally, the residues were washed twice with petroleum ether to give compounds **31**−**33**, pure enough to be used in the next step without purification. Spectroscopic and analytical data for compounds **31**−**33** are in agreement with those reported in the literature.[27]

Method A. General Procedure. Microwave-Assisted Synthesis of Substituted 6-Benzyl-2-(benzylthio)-5-methylpyrimidin-4(3*H*)-ones 3−**6, 8, 11**−**16, 19, and 22**−**28.** Compounds **31**−**33** (0.3 mmol) and appropriate halobenzyl derivatives (0.3 mmol) were suspended in the least amount of dry DMF (0.7 mL) in sealed vessels in the presence (**31**, **33**) or not (**32**) of K_2CO_3 (0.041 g, 0.3 mmol), and the mixtures were irradiated at 130 °C for 5 min. The reaction mixtures were then diluted with water (2 mL) and extracted with ethyl acetate (3 × 10 mL). Finally, the organic phases were dried over anhydrous Na_2SO_4 and evaporated to dryness. The residues were purified by crystallization to give compounds **3**−**6**, **8**, **11**−**16**, **19**, and **22**−**28** in good yields and high purity.

Method A. Examples. 6-(2,6-Dichlorobenzyl)-2-(4-methoxybenzylthio)-5-methylpyrimidin-4(3*H*)-one (8). Yield 72%. Mp 197−199 °C. IR ($CHCl_3$) (ν, cm^{-1}): 841, 920, 1512, 1645, 3018. ^1H NMR (DMSO-d_6): δ 2.02 (s, 3H), 3.66 (s, 3H), 3.91 (s, 2H), 4.17 (s, 2H), 6.62−6.77 (m, 4H), 7.21−7.47 (m, 3H), 12.52 ppm (br, 1H). MS (ESI) *m/z*: 443 $[M + Na]^+$. HPLC (C_8 column; CH_3CN/H_2O, 50/50) t_R 18.08 min. Anal. ($C_{20}H_{18}Cl_2N_2O_2S$) C, H, S; N.

6-(2,6-Dichlorobenzyl)-2-(4-nitrobenzylthio)-5-methylpyrimidin-4(3*H*)-one (13). Yield 55%. Mp 231−232 °C. IR ($CHCl_3$) (ν, cm^{-1}): 1348, 1523, 1647, 3007. ^1H NMR ($CDCl_3$): δ 2.17 (s, 3H), 4.14 (s, 2H), 4.23 (s, 2H), 6.99−7.99 (m, 7H), 11.93 ppm (br, 1H). MS (ESI) *m/z*: 434 $[M - H]^-$. HPLC (C_{18} column; CH_3OH/H_2O, 90/10) t_R 3.58 min. Anal. ($C_{19}H_{15}Cl_2N_3O_3S$) C, H, S; N.

Method B. General Procedure. Microwave-Assisted Synthesis of Substituted 6-Benzyl-2-(benzylthio)-5-methylpyrimidin-4(3*H*)-ones 7, 9, **10**, **17**, **18**, **20**, **21, 29, and 30.** Compounds **31**−**33** (0.3 mmol) and appropriate benzyl alcohol derivatives (0.3 mmol) were suspended in the least amount of dry DMF (1 mL) in the presence of trimethylphosphine (0.3 mL) (1 M solution in toluene). The reaction mixtures were cooled in ice bath, and DIAD was added (0.3 mmol). The mixtures were irradiated at 40° C for 10 min and then were diluted with water (2 mL) and extracted with diethyl ether (5 × 10 mL). Finally, the combined organic phases were dried over anhydrous Na_2SO_4 and evaporated to dryness. The residues were purified on silica gel by flash chromatography and recrystallized by using a suitable solvent, to give compounds **7**, **9**, **10**, **17**, **18**, **20**, **21**, **29**, and **30** in very high purity.

Method B. Examples. 6-(2,6-Dichlorobenzyl)-2-(2-(4-methoxyphenyl)ethylthio)-5-methylpyrimidin-4(3*H*)-one (20). The product was purified by flash chromatography (eluent: CH_2Cl_2/MeOH, 97/3) to give a white solid (yield 53%), which was recrystallized from acetonitrile. Mp 182−183°C. IR ($CHCl_3$) (ν, cm^{-1}): 1539, 1659, 3022. ^1H NMR (DMSO-d_6): δ 2.01 (s, 3H), 2.43 (t, 2H J = 7.27), 2.89 (t, 2H J = 7.26), 3.69 (s, 3H), 4.15 (s, 2H), 6.77−6.89 (m, 4H), 7.17−7.40 (m, 3H), 12.47 (br s, 1H). MS (ESI) *m/z*: 435 $[M + H]^+$, 457 $[M + Na]^+$. HPLC (C_8 column; MeOH/H_2O, 80/20) t_R 7.59 min. Anal. ($C_{21}H_{20}Cl_2N_2O_2S$) C, H, S; N.

6-(2,6-Dichlorobenzyl)-2-(3-(4-methoxyphenyl)propylthio)-5-methylpyrimidin-4(3*H*)-one (21). The product was purified by flash chromatography (eluent: CH_2Cl_2/MeOH, 97/3) to give a white solid (yield 67%), which was recrystallized from acetonitrile. Mp 180−182°C. IR ($CHCl_3$) (ν, cm^{-1}): 1540, 1644, 3018. ^1H NMR (DMSO-d_6): δ 1.45 (quint, 2H J = 7.1), 2.00 (s, 3H), 2.29 (t, 2H J = 7.2), 2.62 (t, 2H J = 6.96), 3.68 (s, 3H), 4.12 (s, 2H), 6.78−6.98 (m, 4H), 7.18−7.41 (m, 3H), 12.50 (br s, 1H). MS (ESI) *m/z*: 449 $[M + H]^+$, 471 $[M + Na]^+$. HPLC (C_8 column; MeOH/H_2O, 80/20) t_R 9.55 min. Anal. ($C_{22}H_{22}Cl_2N_2O_2S$) C, H, S; N.

Parallel Synthesis of Substituted 6-Benzyl-2-(benzylsulfonyl)-5-methylpyrimidin-4(3*H*)-ones (38−**40). General Procedure.** Compounds **6**, **8**, and **13** (0.2 mmol) were placed in four different vessels of the Buchi Syncore and dissolved in 6 mL of dry CH_2Cl_2. A solution of *m*-chloroperbenzoic acid (0.103 g, 0.6 mmol) in dry CH_2Cl_2 (6 mL) was added dropwise in each vessel, and the resulting solutions were shaken overnight at room temperature at 360 rpm. The reaction mixtures were evaporated to dryness in parallel to obtain crude materials that were purified by flash chromatography to afford the final products.

Examples. 6-(2,6-Dichlorobenzyl)-2-(4-methoxybenzylsulfonyl)-5-methylpyrimidin-4(3*H*)-one (38). The product was purified by flash chromatography (eluent: AcOEt/AcOH, 99/1) to give a white solid (yield 71%), which was recrystallized from acetonitrile. Mp 171−174 °C. ^1H NMR ($CDCl_3$): δ 2.31 (s, 3H), 3.73 (s, 3H), 4.32 (s, 2H), 4.41 (s, 2H), 6.65−6.77 (m, 4H), 7.09−7.41 (m, 3H) (m, 7H). MS (ESI) *m/z*: 475 $[M + Na]^+$, 491 $[M + K]^+$. HPLC (C_{18} column; CH_3CN/H_2O, 70/30) t_R 4.36 min. Anal. ($C_{20}H_{18}Cl_2N_2O_4S$) C, H, S; N.

6-(2,6-Dichlorobenzyl)-2-(4-bromobenzylsulfonyl)-5-methylpyrimidin-4(3*H*)-one (39). The product was purified by flash chromatography (eluent: AcOEt/petroleum ether/AcOH, 30/10/0.6) to give a white solid (yield 55%). Mp 241−244 °C. ^1H NMR (DMSO-d_6): δ 1.85 (s, 3H), 4.10 (s, 2H), 4.23 (s, 2H), 6.79−7.60 (m, 7H). MS (ESI) *m/z*: 500 $[M - H]^-$. HPLC (C_{18} column; CH_3OH/H_2O, 75/25) t_R 2.67 min. Anal. ($C_{19}H_{15}Cl_2N_3O_5S$) C, H, S; N.

6-(2,6-Dichlorobenzyl)-2-(4-nitrobenzylsulfonyl)-5-methylpyrimidin-4(3H)-one (40). The product was purified by flash chromatography (eluent: AcOEt/petroleum ether/AcOH, 30/10/0.6) to give a white solid (yield 50%). Mp 175−180 °C. ^1H NMR (DMSO-d_6): δ 1.96 (s, 3H), 4.11 (s, 2H), 4.53 (s, 2H), 7.14−8.00 (m, 7H). MS (ESI) *m/z*: 466 $[M - H]^-$. HPLC (C_{18} column; CH_3OH/H_2O, 75/25) t_R 2.62 min. Anal. ($C_{19}H_{15}BrCl_2N_2O_3S$) C, H, S; N.

Biology. Anti-HIV Reverse Transcriptase Assays. Recombinant RT wt, Lys103Asn, and Tyr181Ile were expressed and purified to >95% purity (as judged by SDS-PAGE), as described,[34] and had specific activities on poly(rA)/oligo(dT) (see below) of 76 570 units/mg (wt), (K103N), (Y181I); 1 unit of DNA polymerase activity corresponds to the incorporation of 1 nmol of dNMP into acid-precipitatable material in 60 min at 37 °C.

RNA-dependent DNA polymerase activity was assayed as follows: a final volume of 25 μL contained buffer A (50 mM Tris-HCl pH 7.5, 1 mM DTT, 0.2 mg/mL BSA, 4% glycerol), 10 mM $MgCl_2$, 0.5 μg of poly(rA)/oligo(dT)$_{10:1}$ (0.3 μM 3′-OH ends), 10 μM [^{3}H]-dTTP (1 Ci/mmol), and 5−10 nM RT.

Reactions were incubated for 10 min at 37 °C. Aliquots (20 μL) were then spotted on glass fiber filters GF/C, which were immediately immersed in 5% ice-cold TCA. Filters were washed twice in 5% ice-cold TCA and once in ethanol for 5 min. Incorporation of radioactive dTTP into poly(rA)/oligo(dT) at different concentrations of DNA or dNTP was monitored in the presence of increasing amounts of inhibitor.

Anti-HIV Activity in Lymphoid Cells. Biological activity of the compounds was tested in the lymphoid MT-4 cell line (received from the NIH AIDS Reagent Program) against the wt HIV-1 NL4-3 strain and three different HIV-1 strains, as described before.[35] Briefly, MT-4 cells were infected with the appropriate HIV-1 strain (or mock-infected to determine cytotoxicity) in the presence of different drug concentrations. At day five post-infection, a tetrazolim-based colorimetric method (MTT method) was used to evaluate the number of viable cells. The IRLL98 HIV-1 strain contains the following mutations in the RT coding sequence:[36] M41L, D67N, Y181C, M184V, R211K, T215Y (conferring resistance to NRTI) and mutations K101Q, Y181C, G190A (conferring resistance to NNRTI). The HIV-1 strains containing the multi-NNRTI mutation, K103N, or the Y188L mutant were received from the Medical Research Council Centralised Facility for AIDS Reagents, Herfordshire, UK.

Computational Details. All calculations and manipulations were performed using Autodock 3.0[37] and Macromodel 8.5[38]/Maestro,[39] running on Silicon Graphics Octane R12000 and IBM Intel Xeon workstations. Amber force field was used for minimization procedures as implemented in the Macromodel software package.

Three-dimensional coordinates of the HIV-1 RT/MKC-442 (emivirine) complex (Brookhaven Protein Data Bank entry 1RT1) were used as the input structure for docking calculations. For this aim, all cocrystallized water molecules were deleted, and all polar hydrogens were added using the appropriate tool in the builder module of Maestro. The structures of the new *S*-DABO derivatives were built using the Maestro 3D-sketcher and fully minimized (Polak-Ribiere conjugate gradient of 0.05 kJ/Å mol convergence). Atom charges assigned to compounds during the minimization step were retained for the following docking calculation.

For molecular docking purposes, a box of 64 × 50 × 62 points was set that comprised all residues constituting the NNRTI binding pocket. Starting structures of the selected compounds were randomly defined to obtain totally unbiased results. The genetic algorithm-local search (GA-LS) method was used with the default settings and retrieved 100 docked conformations from each compound. Results from Autodock calculations were clustered using an RMSD tolerance of 2 Å and the lowest energy conformer of the most populated cluster (the lowest energy cluster in most cases) was selected as the most probable binding conformer. HIV-1 RT/ligand complexes were submitted to a full minimization of the whole structure to a 0.1 kJ/Å mol gradient.

Acknowledgment. This study was partially supported by grants from the European TRIoH Consortium (LSHB-2003-503480), the Fundació La Marató de TV3 project 020930 (J.A.E.), and the Spanish Ministerio de Ciencia y Tecnología project BFI-2003-00405 (J.A.E.). G.M. was supported by the ISS-National Research Program on AIDS (Grants 40F.78 and 40F.48). C.C. thanks the Dipartimento Farmaceutico, Università degli Studi di Parma, for a leave to work at the Dipartimento Farmaco Chimico Tecnologico, Università degli Studi di Siena. M.B. thanks the Merk Research Laboratories (2004 Academic Development Program Chemistry Award). F.M. thanks the Divisione di Chimica Farmaceutica della Società Chimica Italiana and Farmindustria for the "Premio Farmindustria 2004" award.

Supporting Information Available: Details of synthesis and elemental analysis data. This material is available free of charge via the Internet at http://pubs.acs.org.

References

(1) St. Clair, M. H.; Richards, C. A.; Spector, T.; Weinhold, K. J.; Miller, W. H.; Langlois, A. J.; Furman, P. A. 3′-Azido-3′-deoxythymidinetriphosphate as an Inhibitor and Substrate of Purified Human Immunodeficiency Virus Reverse Transcriptase. *Antimicrob. Agents Chemother.* **1987**, *31,* 1972−1977.

(2) Merluzzi, V. J.; Hargrave, K. D.; Labadia, M.; Grozinger, K.; Skoog, M.; Wu, J. C.; Shih, C.-K.; Eckner, K.; Hattox, S.; Adams, J.; Rosenthal, A. S.; Faanes, R.; Eckner, R. J.; Koup, R. A.; Sullivan, J. L. Inhibition of HIV-1 Replication by a Nonnucleoside Reverse Transcriptase Inhibitor. *Science* **1990**, *250,* 1411−1413.

(3) Pauwels, R.; Andries, K.; Desmyter, J.; Schols, D.; Kukla, M. J.; Breslin, H. J.; Rayemaeckers, A.; Gelder, J. V.; Woestenborghs, R.; Heykants, J.; Schellekens, K.; Janssen, M. A. C.; De Clercq, E.; Janssen, P. A. J. Potent and Selective Inhibition of HIV-1 Replication in Vitro by a Novel Series of TIBO Derivatives. *Nature* **1990**, *343,* 470−474.

(4) Romero, D. L.; Busso, M.; Tan, C.-K.; Reusser, F.; Palmer, J. R.; Poppe, S. M.; Aristoff, P. A.; Downey, K. M.; So, A. G.; Rasnick, L.; Tarpley, W. G. Nonnucleoside Reverse Transcriptase Inhibitors That Potently and Specifically Block Human Immunodeficiency Virus Type 1 Replication. *Proc. Natl. Acad. Sci. U.S.A.* **1991**, *88,* 8806−8810.

(5) Pauwels, R.; Andries, K.; Debyser, Z.; Van Daele, P.; Schols, D.; Stoffels, P.; De Vreese, K.; Woestenborghs, R.; Vandamme, A.-M.; Janssen, C. G. M.; Anne, J.; Cauwenbergh, G.; Desmyter, J.; Heykants, J.; Janssen, M. A. C.; De Clercq, E.; Janssen, P. A. J. Potent and High Selective HIV-1 Inhibition by a New Series of R-Anilinophenylacetamide R-APA Derivatives Targeted at HIV-1 Reverse Transcriptase. *Proc. Natl. Acad. Sci. U.S.A.* **1993**, *90,* 1711−1715.

(6) Cantrell, A. S.; Engelhardt, P.; Hogberg, M.; Jaskunas, S. R.; Johansson, N. G.; Jordan, C. L.; Kangasmetsa, J.; Kinnick, M. D.; Lind, P.; Morin, J. M., Jr.; Muesing, M. A.; Noreen, R.; Oberg, B.; Prane, P.; Sahlberg, C.; Ternasky, R. J.; Vasileff, R. T.; Vrang, L.; West, S. J.; Zhang, H. Phenethylthiazolylthiourea (PETT) Compounds as a New Class of HIV-1 Reverse Transcriptase Inhibitors. 2. Synthesis and Further Structure−Activity Relationship Studies of PETT Analogues. *J. Med. Chem.* **1996**, *39*, 4261−4274.

(7) Baba, M.; Tanaka, H.; De Clercq, E.; Pauwels, R.; Balzarini, J.; Schols, D.; Nakashima, H.; Perno, C.-F.; Walker, R. T.; Miyasaka, T. Highly Specific Inhibition of Human Immunodeficiency Virus Type-1 by a Novel 6-Substituted Acyclouridine Derivative. *Biochem. Biophys. Res. Commun.* **1989**, *165,* 1375−1381.

(8) Hopkins, A. L.; Ren, J.; Esnouf, R. M.; Willcox, B. E.; Jones, E. Y.; Ross, C.; Miyasaka, T.; Walker, R. T.; Tanaka, H.; Stammers, D. K.; Stuart, D. I. Complexes of HIV-1 Reverse Transcriptase with Inhibitors of the HEPT Series Reveal Conformational Changes Relevant to the Design of Potent Non-Nucleoside Inhibitors. *J. Med. Chem.* **1996**, *39*, 1589−1600.

(9) Ludovici, D. W.; Kukla, M. J.; Grous, P. G.; Krishnan, S.; Andries, K.; et al. Evolution of Anti-HIV Drug Candidates. Part 1: From R-Anilinophenylacetamide (R-APA) to Imidoyl Thiourea (ITU). *Bioorg. Med. Chem. Lett.* **2001**, *11*, 2225−2228.

(10) Ludovici, D. W.; Kavash, R. W.; Kukla, M. J.; Ho, C. Y.; Ye, H.; et al. Evolution of Anti-HIV Drug Candidates Part 2: Diarylpyrimidine (DATA) Analogues. *Bioorg. Med. Chem. Lett.* **2001**, *11*, 2229−2234.

(11) Das, K.; Clark, A. D., Jr.; Lewi, P. J.; Heeres, J.; de Jonge, M. R.; Koymans, L. M. H.; Vinkers, H. M.; Daeyaert, F.; Ludovici, D. W.; Kukla, M. J.; De Corte, B.; Kavash, R. W.; Ho, C. Y.; Ye, H.; Lichtenstein, M. A.; Andries, K.; Pauwels, R.; de Béthune, M. P.; Boyer, P. L.; Clark, P.; Hughes, S. H.; Janssen, P. A. J.; Arnold, E. Roles of Conformational and Positional Adaptability in Structure-Based Design of TMC125-R165335 (Etravirine) and Related Non-nucleoside Reverse Transcriptase Inhibitors That Are Highly Potent and Effective against Wild-Type and Drug-Resistant HIV-1 Variants. *J. Med. Chem.* **2004,** *47,* 2550−2560.

(12) Guillemont, J.; Pasquier, E.; Palandjian, P.; Vernier, D.; Gaurrand, S.; Lewi, P. J.; Heeres, J.; de Jonge, M. R.; Koymans, L. M. H.; Daeyaert, F. F. D.; Vinkers, M. H.; Arnold, E.; Das, K.; Pauwels, R.; Andries, K.; de Béthune, M. P.; Bettens, E.; Hertogs, K.; Wigerinck, P.; Timmerman, P.; Janssen, P. A. J. Synthesis of Novel Diarylpyrimidine Analogues and Their Antiviral Activity against Human Immunodeficiency Virus Type 1. *J. Med. Chem.* **2005**, *48*, 2072−2079.

(13) Janssen, P. A. J.; Lewi, P. J.; Arnold, E.; Daeyaert, F.; de Jonge, M.; Heeres, J.; Koymans, L.; Vinkers, M.; Guillemont, J.; Pasquier, E.; Kukla, M.; Ludovici, D.; Koen, A.; de Béthune, M. P.; Pauwels, R.; Das, K.; Clark, A. D., Jr.; Frenkel, Y. V.; Hughes, S. H.; Medaer, B.; De Knaep, F.; Bohets, H.; De Clerck, F.; Lampo, A.; Williams, P.; Stoffels, P. In Search of a Novel Anti-

HIV Drug: Multidisciplinary Coordination in the Discovery of 4-[[4-[(1*E*)-2-Cyanoethenyl]-2,6-dimethylphenyl]amino]-2-pyrimidinyl]amino]benzonitrile (R278474, Rilpivirine). *J. Med. Chem.* **2005**, *48*, 1901−1909.
(14) Ren, J.; Esnouf, R.; Garman, E.; Somers, D.; Ross, C.; Kirby, I.; Keeling, J.; Darby, G.; Jones, Y.; Stuart, D.; Stammers, D. High-Resolution Structures of HIV-1 RT from Four RT-Inhibitor Complexes. *Nat. Struct. Biol.* **1995**, *2,* 293−302.
(15) Smerdon, S. J.; Jager, J.; Wang, J.; Kohlstaedt, L. A.; Chirino, A. J.; Friedman, J. M.; Rice, P. A.; Stetz, T. A. Structure of the Binding Site for Nonnucleoside Inhibitors of the Reverse Transcriptase of Human Immunodeficiency Virus Type 1. *Proc. Natl. Acad. Sci. U.S.A.* **1994**, *91,* 3911−3915.
(16) Ding, J.; Das, K.; Tantillo, C.; Zhang, W.; Clark, A. D., Jr.; Jessen, S.; Lu, X.; Hsiou, Y.; Jacobo-Molina, A.; Andries, K.; Pauwels, R.; Moereels, H.; Koymans, L.; Janssen, P. A. J.; Smith, R. H., Jr.; Kroeger Koepke, M.; Michejda, C. J.; Hughes, S. H.; Arnold, E. Structure of HIV-1 Reverse Transcriptase in a Complex with the Non-Nucleoside Inhibitor α-APA R 95 845 at 2.8 Å Resolution. *Structure* **1995**, *3,* 365−379.
(17) Ren, J.; Esnouf, R.; Hopkins, A.; Ross, C.; Jones, Y.; Stammers, D.; Stuart, D. The Structure of HIV-1 Reverse Transcriptase Complexed with 9-Chloro-TIBO: Lessons for Inhibitor Design. *Structure* **1995**, *3,* 915−926.
(18) Das, K.; Ding, J. P.; Hsiou, Y.; Clark, A. D.; Moereels, H.; Koymans, L.; Andries, K.; Pauwels, R.; Janssen, P. A. J.; Boyer, P. L.; Clark, P.; Smith, R. H.; Smith, M. B. K.; Michejda, C. J.; Hughes, S. H.; Arnold, E. Crystal Structures of 8-Cl and 9-Cl TIBO Complexed with Wild-Type HIV-1 RT and 8-Cl TIBO Complexed with the Tyr181Cys HIV-1 RT Drug-Resistant Mutant. *J. Mol. Biol.* **1996**, *264,* 1085−1100.
(19) Esnouf, R. M.; Ren, J. S.; Hopkins, A. L.; Ross, C. K.; Jones, E. Y.; Stammers, D. K.; Stuart, D. I. Unique Features of the Complex between HIV-1 Reverse Transcriptase and the Bis-(heteroaryl)piperazine (BHAP) U-90152 Explain Resistance Mutations for this Nonnucleoside Inhibitor. *Proc. Natl. Acad. Sci. U.S.A.* **1997**, *94,* 3984−3989.
(20) Ren, J.; Esnouf, R. M.; Hopkins, A. L.; Warren, J.; Balzarini, J.; Stuart, D. I.; Stammers, D. K. Crystal Strucutures of HIV-1 Reverse Transcriptase in Complex with Carboxanilide Derivatives. *Biochemistry* **1998**, *37*, 14394−14403.
(21) Högberg, M.; Sahlberg, C.; Engelhardt, P.; Noréen, R.; Kangasmetsä, J.; Johnsson, N. G.; Öberg, B.; Vrang, L.; Zhang, H.; Sahlberg, B.-L.; Unge, T.; Lövgren, S.; Fridborg, K.; Bäckbro, K. Urea-PETT Compounds as a New Class of HIV-1 Reverse Transcriptase Inhibitors. 3. Synthesis and Further Structure−Activity Relationship Studies of PETT Analogues. *J. Med. Chem.* **1999**, *42,* 4150−4160.
(22) Arnold, E.; Das, K.; Ding, J.; Yadav, P. N. S.; Hsiou. Y.; Boyer, P.; Hughes, S. H. Targeting HIV Reverse Trascriptase for Anti-AIDS Drug Design: Structural and Biological Considerations for Chemotherapeutic Strategies. *Drug. Des. Discovery* **1996**, *13*, 29−47.
(23) De Clercq, E. Toward Improved Anti-HIV Chemotherapy: Therapeutic Strategies for Intervention with HIV Infections. *J. Med. Chem.* **1995**, *38,* 2491−2517.
(24) De Clercq, E. Antiviral Therapy for Human Immunodeficiency Virus Infections. *Clin. Microbiol. Rev.* **1995**, *8,* 200−239.
(25) Botta, M.; Artico, M.; Massa, S.; Gambacorta, A.; Marongiu, M. E.; Pani, A.; La Colla, P. Synthesis, Antimicrobial and Antiviral Activities of Isotrimethoprim and Some Related Derivatives. *Eur. J. Med. Chem.* **1992**, *27*, 251−257.
(26) Parlato, M. C.; Mugnaini, C.; Renzulli, M. L.; Corelli, F.; Botta, M. Solid-Phase Synthesis of 5,6-Disubstituted Pyrimidinone and Pyrimidindione Derivatives. *ARKIVOC* **2004**, *v*, 349−363.
(27) Mai, A.; Artico, M.; Sbardella, G.; Massa, S.; Novellino, E.; Greco, G.; Loi, A. G.; Tramontano, E.; Marongiu, M. E.; La Colla, P. 5-Alkyl-2-(alkylthio)-6-(2,6-dihalophenylmethyl)-3,4-dihydropyrimidin-4(3H)-ones: Novel Potent and Selective Dihydro-alkoxybenxyl-oxopyrimidine Derivatives. *J. Med. Chem.* **1999**, *42*, 619−627.
(28) Radi, M.; Petricci, E.; Maga, G.; Corelli, F.; Botta, M. Parallel Solution Phase Synthesis of 4-Dialckylamino-2-methylsulfonyl-6-vinylpyrimidines. *J. Comb. Chem.* **2005**, *7*, 117−122.
(29) Clay, R. J.; Collom, T. A.; Karrick, G. L.; Wemple, J. A. Safe, Economical Method for the Preparation of β-Oxo Esters. *Synthesis* **1993**, 290−292.
(30) Petricci, E.; Mugnaini, C.; Radi, M.; Corelli, F.; Botta, M. Microwave-Assisted Acylation of Amines, Alcohols, and Phenols by the Use of Solid-Supported Reagents (SSRs). *J. Org. Chem.* **2004**, *69*, 7880−7887.
(31) Obrecht, D.; Abrecht, C.; Grieder, A.; Villalgordo, J. M. A Novel and Efficient Approach for the Combinatorial Synthesis of Structurally Diverse Pyrimidines on Solid Support. *Helv. Chim. Acta* **1997**, *80*, 65−71.
(32) Mai, A.; Artico, M.; Ragno, R.; Sbardella, G.; Massa, S.; Musiu, C.; Mura, M.; Marturana, F.; Cadeddu, A.; Maga, G.; La Colla, P. 5-Alkyl-2-alkylamino-6-(2,6-difluorophenylalkyl)-3,4-dihydropyrimidin-4(3H)-ones, A New Series of Potent, Broad-Spectrum Nonnucleoside Reverse Transcriptase Inhibitors Belonging to the DABO Family. *Bioorg. Med. Chem.* **2005**, *13*, 2065−2077, and references therein.
(33) Box, V. G. S.; Marinovich, N.; Yiannikouros, G. P. The Synthesis of β-Lactones and β-Lactams from Malonates and Malonamides. *Heterocycles* **1991**, *2*, 245−251.
(34) Maga, G.; Amacker, M.; Ruel, N.; Hubscher, U.; Spadari S. Resistance to Nevirapine of HIV-1 Reverse Transcriptase Mutants: Loss of Stabilizing Interactions and Thermodynamic or Steric Barriers are Induced by Different Single Amino Acid Substitutions. *J. Mol. Biol.* **1997**, *274*, 738−47.
(35) Armand-Ugon, M.; Gutierrez, A.; Clotet, B.; Este, J. A. HIV-1 Resistance to the gp41-Dependent Fusion Inhibitor C-34. *Antiviral Res.* **2003**, *59*, 137−142.
(36) Cabana, M.; Clotet, B.; Martinez, M. A. Emergence and Genetic Evolution of HIV-1 Variants with Mutations Conferring Resistance to Multiple Reverse Transcriptase and Protease Inhibitors. *J. Med. Virol.* **1999**, *59*, 480−90.
(37) Goodsell, D. S.; Morris, G. M.; Olson, A. J. Automated Docking of Flexible Ligands: Applications of AutoDock. *J. Mol. Recognit.* **1996**, *9*, 1−5.
(38) Mohamadi, F.; Richards, N. G. J.; Guida, W. C.; Liskamp, R.; Lipton, M.; Caufield, C.; Chang, G.; Hendrickson, T.; Still, W. C. MacroModel-An Integrated Software System for Modeling Organic and Bioorganic Molecules Using Molecular Mechanics. *J. Comput. Chem.* **1990**, *11*, 440−467.
(39) Maestro, version 6.0, is distributed by Schroedinger.

JM050744T